International Journal of Engineering Research and Development

DOI: 10.29137/ijerad.1635246

Volume:17 Issue:2 Pages:472-497 July/2025

Research Article

Investigation of The Effectiveness of Blasting Patterns in Tunnel Excavations: The Case of The Sarıyer - Kilyos Tunnel

Meltem Doğan Karaca [1], **Suleyman Onur Karaca** [1], **Osman Murat Sarsılmaz** [2]

[1]Atakent Mh. Prf Aziz Ergin Cd., Kucukcekmece, 34307 Istanbul, TURKIYE
[2]Yıldızevler Mh. Duyu Cd. Cankaya, 06550 Ankara, TURKIYE

Received: 08/02/2025 **Accepted**: 22/05/2025 **Published Online:**01/07/2025
Final Version: 15/07/2025

Abstract

This study aims to explain the geological structure, soil surveys, and rock classes predicted during the design phase for NATM tunnels located on main alignment, in order to compare the rock classes encountered during construction with those predicted. It also proposes blasting design solutions based on tunnel face data to address issues experienced during blasting pattern application. The study includes alignment data, tunnel section, geology and geotechnical parameters, excavation support analysis methods, support element applications, drainage systems, predicted blasting patterns, and optimal blasting designs based on trial blasts. The findings highlight the differences between the predicted and encountered rock classes during excavation. Therefore, it reveals how crucial the tunnel face mapping is at each excavation step. The study demonstrates that the blasting pattern and temporary support elements might be edited at each excavation step according to location, spacing, and angle of discontinuity, bedding plane, weathering degree, etc., even if the excavation proceeds in the same rock class. The impact of design changes on blasting performance, costs, preparation, blasting, and excavation removal times are also shown. Analyses based on critical geotechnical conditions and overburden height for excavation support classes determined for each rock class demonstrate that excavation support elements safely withstand loads per Eurocode standards. It was shown that varying overburden heights yield different safety factors for the same excavation support system, indicating that support classes must be evaluated based on the overburden height of the application area.

Keywords

NATM Rock Class, Temporary Support System, Drill Blast System, Blasting Material, Blasting Pattern Design, Tunnel Boring Machine.

***Corresponding Author:** meltemdogan2010@gmail.com*

1. Introduction

The Sarıyer-Kilyos road tunnel and connecting routes extend in a north-south direction, starting from the Sarıyer district towards the Kilyos neighborhood. Located on the European side of Istanbul, this project aims to reduce urban traffic between Sarıyer and Kilyos, save time and fuel, and provide an important transportation route in emergency or disaster situations. Additionally, it connects Sarıyer and its surrounding traffic to the high-standard Northern Marmara Highway (KMO) and facilitates fast and comfortable access to the Istanbul Strait via the Uskumruköy Junction and the Sarıyer-Kilyos tunnel for journeys from the Asian side to Istanbul. The project location and the geometric characteristics of the tunnel alignment are shown in Figure 1.

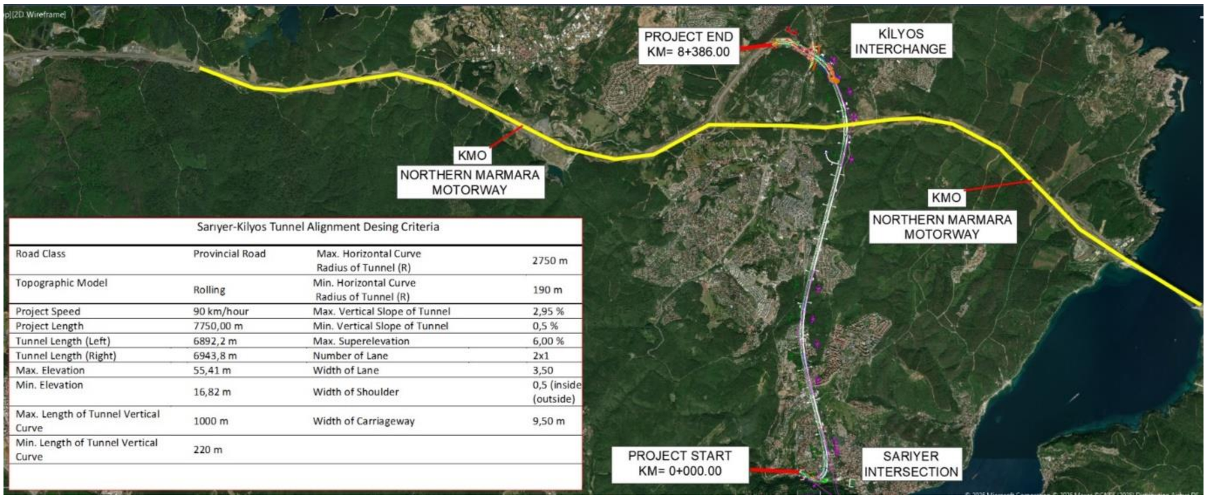

Sarıyer-Kilyos Tunnel Alignment Desing Criteria

Road Class	Provincial Road	Max. Horizontal Curve Radius of Tunnel (R)	2750 m
Topographic Model	Rolling	Min. Horizontal Curve Radius of Tunnel (R)	190 m
Project Speed	90 km/hour	Max. Vertical Slope of Tunnel	2,95 %
Project Length	7750,00 m	Min. Vertical Slope of Tunnel	0,5 %
Tunnel Length (Left)	6892,2 m	Max. Superelevation	6,00 %
Tunnel Length (Right)	6943,8 m	Number of Lane	2x1
Max. Elevation	55,41 m	Width of Lane	3,50
Min. Elevation	16,82 m	Width of Shoulder	0,5 (inside (outside)
Max. Length of Tunnel Vertical Curve	1000 m	Width of Carriageway	9,50 m
Min. Length of Tunnel Vertical Curve	220 m		

Figure 1. Project location and tunnel Alignment.

The project includes one junction arrangement, two cut-and-cover structures, one portal, a twin-tube tunnel in the southern region, and one portal, two cut-and-cover structures, one culvert, one viaduct, and one junction arrangement in the northern region. Additionally, a cavern structure is planned near the midpoint of the left and right tubes for TBM assembly. The excavation of the cavern on the left tube has been completed using the NATM method, and preparations are underway for the cavern on the right tube. A 400-meter-long approach tunnel has also been excavated in the left tube to support NATM excavation works logistically and mobilization-wise. This study focuses on the temporary support systems and blasting patterns applied during the construction of the NATM tunnels (4230 meters in the northern region) on the main route, which have been completed with a 2x2 lane configuration and a traffic lane width of 9.5 meters. The typical cross-section of the NATM main tunnel is shown in Figure 2.

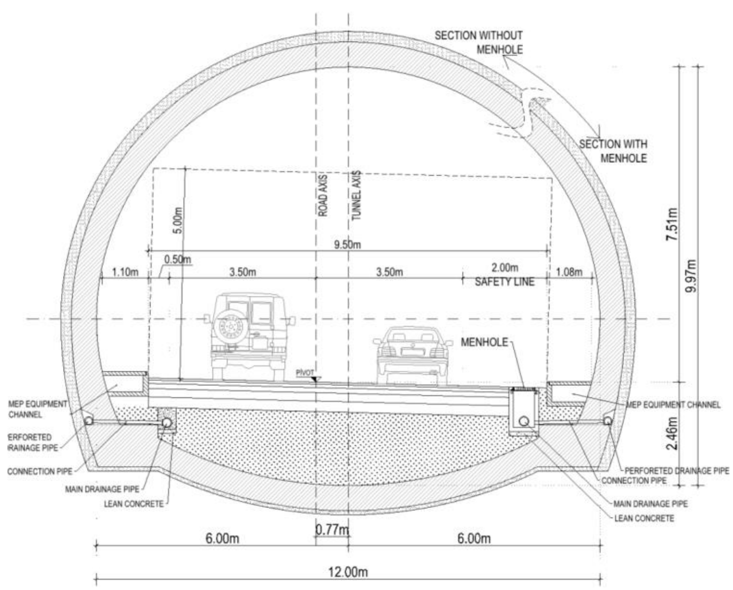

Figure 2. Main Tunnel Type Cross Section.

The tunnel, which will serve as a significant connection route in such a crucial location, will have a total length of 13,836 meters upon completion, making it one of the notable tunnels constructed in the city center. The tunnel geology consists of the Trakya Formation and the Garipçe Formation. The Trakya Formation is located in the southern region of the tunnel, approximately within the first 500 meters, characterized by a weak to moderately strong alternation of greywacke-dominated sandstone and shale. The Garipçe Formation comprises highly to completely weathered granular tuff and cataclastic rocks at tunnel depth in the southern region, and medium to high-strength pyroclastic rocks containing andesite and basaltic andesite in the northern region. Therefore, it has been decided to apply the NATM method for the first 500 meters in the south and 4230 meters in the north, where the geological units to be excavated have high strength, low weathering degree, and relatively lower overburden, and the TBM method for 8750 meters in the southern region, where the geological units to be excavated have low strength, high weathering degree, high groundwater table and high overburden.

Several limitations on the choice of excavation methods NATM and TBM can be listed as follows:

Limitations of the NATM Excavation Method:

- In weak/highly deformable ground conditions, substantial temporary support systems are required to stabilize the tunnel until the final lining is installed.
- These robust temporary supports significantly increase construction costs and reduce advance rates.
- The method typically necessitates the excavation of several adit tunnels from the surface to facilitate mobilization, logistics, and the disposal of excavated material from additional tunnel excavation teams to increase the advance rate.
- In relatively competent rock formations, NATM allows for the use of drill-and-blast techniques as an alternative to mechanized excavation.
- Drill-and-blast methods can offer high excavation rates where permissible, thus reducing the overall construction duration.
- In zones where explosive techniques are employed, it is imperative to adhere to an extensive regulatory framework. This framework necessitates the initial approval to avoid any delay of first drill-blast operation and subsequent periodic renewal of blasting permits. The synchronization of this process with the project timeline is crucial, requiring compliance with an array of jurisdictional and governmental regulations.
- Measurements of vibration and air overpressure after each blast are required to meet environmental and safety standards under local and international regulations, including the International Finance Corporation PS1-8 policies.
- In proximity to sensitive surface structures, it may be necessary to revise blast patterns and charge configurations to mitigate risk.

Limitations of the TBM Excavation Method:

- In weak/highly deformable ground conditions, substantial temporary support systems are required to stabilize the tunnel until the final lining is installed.
- These robust temporary supports significantly increase construction costs and reduce advance rates.
- The method typically necessitates the excavation of several adit tunnels from the surface to facilitate mobilization, logistics, and the disposal of excavated material from additional tunnel excavation teams to increase the advance rate.
- In relatively competent rock formations, NATM allows for the use of drill-and-blast techniques as an alternative to mechanized excavation.
- Drill-and-blast methods can offer high excavation rates where permissible, thus reducing the overall construction duration.

In a study by Çümen and Karakaş (2021), the geological and geotechnical structure of The Kınık Tunnel on the Erzurum-Rize highway route was examined, and rock classification according to the NATM method was performed, along with a discussion of the applied excavation support systems. In another study by Furat and Bulut (2020), the entrance and exit sections of the Güneyce Tunnel on the Rize-İspir highway route, constructed using the drill-and-blast method, were analyzed using different rock classification methods, and proposed tunnel support types were examined. In a study by Kahyaoğlu (1998), the excavation support systems of tunnels constructed using the NATM method in the third section of the Adana-Toprakkale-Gaziantep highway near the Bahçe district were reviewed.

In the study by Çoruh et al. (2017) titled "Kop Tunnel Construction Works and Methodology," the excavation methods included mechanized excavation, drill-and-blast, and TBM, but the performance of drill-and-blast in areas where it was applied was not discussed. In the study by Hiçyılmaz and Özçelik (2019) titled "Ankara-Sivas High-Speed Railway Project T-5 Tunnel Construction Works," the excavation and support system of a tunnel excavated using the NATM method were examined, and issues encountered in the drill-and-blast section due to the presence of decomposed clayey agglomerate were discussed. In the article by Singh and Xavier (2004) titled "Causes, Impact, and Control of Overbreak in Underground Excavations," the relationship between rock mechanical properties and blasting performance was studied. In the study by Alğın et. al. (2019), Avcı and Ekmen (2023), Ekmen and Avcı (2023) the important points related to mesh system selection and convergence studies are explained for the numerical analysis of geotechnical calculations.

In addition, the study utilized numerical models that account for soil-structure interaction for tunnel linings. In the study by Baş (2019) investigates the effects of vertical earthquake excitation on reinforced concrete frame structures, comparing Soil-Structure Interaction (SSI) and fixed support models through engineering parameters, highlighting that incorporating Soil Structure Interaction in analysis is recommended for more reliable results.

Symbols and Abbreviations

KGM	General Directorate of Highways
KMO	Northern Marmara Highway
PPP	Public-Private Partnership Projects
BOT	Build-Operate Transfer
NATM	New Austrian Tunneling Method
TBM	Tunnel Boring Machine
SPT	Standard Penetration Test
MASW	Multichannel Analysis of Surface Waves
WPT	Water Pressure Test
PPV	Particle Peak Velocity
SD	Scaled Distance
RMR	Rock Mass Rating
GSI	Geological Strength Index
UCS	Uniaxial Compressive Strength
m_i	Rock Mass Coefficient
D	Disturbance Factor
E_i	Intact Rock Elastic Modulus
γ	Unit Weight
c	Soil Cohesion
φ	Soil Frictional Angle
E	Soil Elastic Modulus
Z	Overburden Layer Above Tunnel
F_s	Factor of Safety
τ_{m2}	The Average Shear Stress Acting on The Surface of Wedge 2
τ_{m3}	The Average Shear Stress Acting on The Surface of Wedge 3
a	Excavation length
b	Tunnel Width
h	Tunnel Height
k_A	Active Thrust Coefficient
k_A	Passive Thrust Coefficient
P_E	Pressure Applied to The Tunnel Face
R_{core}	Soil Strength Ahead of The Tunnel Face
R_p	The Radius of The Plastic Zone Formed Around the Tunnel
Re	The Radius of The Equivalent Circle of The Tunnel Excavation Area

2. Geological Investigations

The study area is located on one of the main tectonic units of Türkiye, known as the Istanbul Zone (see Figure 3).

Figure 3. Location of the Istanbul Zone within the tectonic units of Türkiye (Aral & Tüysüz, 1999).

Various boreholes with depths ranging from 20 meters to 192 meters were drilled as part of the preliminary application projects. Based on the boreholes and subsequent in-situ and laboratory tests, geological, geotechnical, and hydrogeological information specific to the project was compiled, and rock classification was performed according to ÖNORM B2203 (see Table 1). Temporary support classes were determined using of the Highway Technical Specifications (KTŞ, 2013). Although application details for excavation support systems related to rock classes A2, B1, B2, B3, C2, and C3 have been determined, the part to be examined in this study includes the support systems for rock classes B1, B2, B3, and C2, which have been implemented in the construction site.

Table 1. ÖNORM Rock Classification System

Rock Class		ÖNORM B2203 (October 1994 and later)		ÖNORM B2203 (October 1994 and before)
A	A1	Stable	A1	Stable
	A2	Over-breaking	A2	Local Instabilities
B	B1	Friable	B1	Friable
	B2	Very friable	B2	Very friable
	B3	Rolling		
C	C1	Rock bursting	C1	Squeezing
	C2	Squeezing		
	C3	Heavily squeezing	C2	Heavily squeezing
	C4	Flowing	L1	Loose Soil High Cohesion
	C5	Swelling	L2	Loose Soil Low Cohesion

Three main geological formations were observed along the tunnel alignment:

1. Trakya Formation (Ct)
2. Garipçe Formation (Ksg)
3. Istanbul Formation (Ti)

The section of the NATM main tunnel corresponding to the northern portal is covered with artificial clay fill, while the other sections are located on the İstanbul formation (Ti), and the Garipçe formation (KsgA) is present at the base. In the northern section, the Istanbul Formation above the tunnel level generally consists of loosely cemented, variegated sandstone, siltstone, and conglomerate, with occasional clay layers. The Garipçe Formation is represented by lavas and pyroclastic rocks, with massive andesites exhibiting varying degrees of weathering (Figure 4).

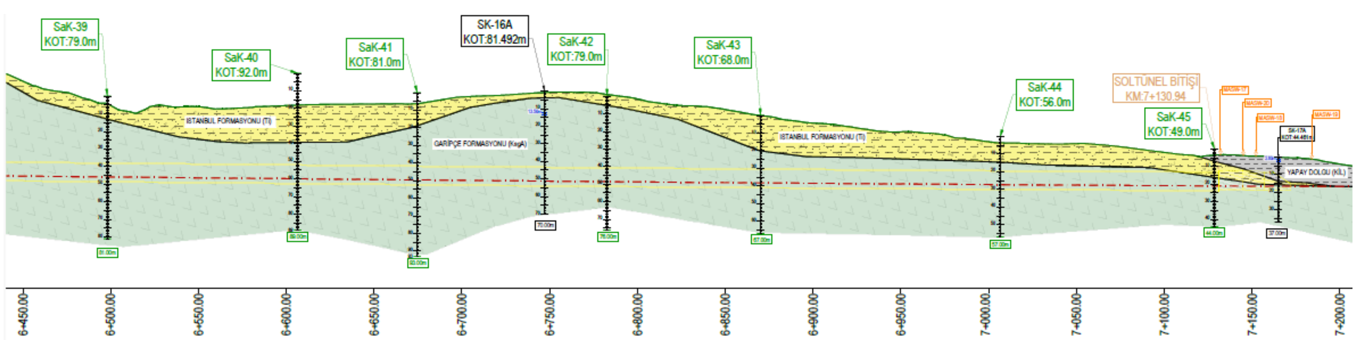

Figure 4. Northern portal section, formation units.

Following the borehole studies within the study area, in-situ and laboratory tests were completed, and geotechnical parameters for the analyzed sections were determined. In the site, Standard Penetration Tests (SPT), pressure meter tests, Multichannel Analysis of Surface Waves (MASW), borehole seismic tests (PS logging), vibrating wire piezometers, water pressure tests (WPT), aquifer tests, and laboratory tests such as uniaxial compressive strength, swelling pressure, uniaxial compressive strength and elasticity modulus, water content, triaxial compressive strength, point load strength index, natural moisture content, Cherchar abrasion test, one-dimensional consolidation, water absorption (apparent porosity), soil classification, direct shear box test, Atterberg limits, triaxial compressive strength, hydrometer free compressive strength, swelling percentage, slake durability index, relative density, and natural unit weight were conducted. Based on these tests, geotechnical parameters for different rock classes in the northern region, dominated by the Garipçe Formation, were selected using the RocLab (2007) program, as summarized in Table 2.

Table 2. Summary of Geotechnical Parameters for the Northern Portal Region

Excavation Support Class	Overburden Height	Units	Layer Thickness	Hoek-Brown Parameters					Mohr-Coulomb Parameters			
				GSI	UCS	m_i	D	E_i	γ	c	φ	E
(-)	(m)	(-)	(m)	(-)	(Mpa)	(-)	(-)	(Gpa)	(kN/m^3)	(Kpa)	(°)	(Mpa)
A2	80	Istanbul Formation	0 - 5	-	-	-	-	-	20	10	29	20
		Garipçe Formation (KsgA-U2C)	>5	60	15	25	0	7.0	24	460	53	3640
							0.5		24	384	48	1900
B3	85	Istanbul Formation	0 - 40	-	-	-	-	-	20	10	29	20
		Garipçe Formation (KsgA-U2C)	>40	30	10	25	0	7.0	24	190	42	560
C2	85	Istanbul Formation	0 - 40	-	-	-	-	-	20	10	29	20
		Garipçe Formation (KsgA-U2C)	>40	20	5	25	0	5.0	22	155	31	300
B2	60	Istanbul Formation	0 - 7	-	-	-	-	-	20	10	29	20
		Garipce Formation (KsgA-U2D)	>7	40	30	25	0	15.0	25	358	53	2390
							0.5		25	279	48	1150
B1	60	Istanbul Formation	0 - 7	-	-	-	-	-	20	10	29	20
		Garipce Formation (KsgA-U2D)	>7	50	30	25	0	10.0	25	436	56	3000
							0.5		25	348	52	1400
A2	40	Istanbul Formation	0 - 10	-	-	-	-	-	20	10	29	20
		Weathered Andesite	10 - 18	20	10	25	0	5.0	24	61	49	200
		Garipçe Formation (KsgA-U2E)	>18	60	30	25	0	10.0	25	459	61	5200
							0.5		25	363	57	2700

3. NATM Temporary Lining Design Criteria

The three basic design principles followed in the NATM used in tunnel design calculations can be listed as follows:

1. Utilization of the Ground-Rock Mass's Bearing Capacity: NATM aims to maximize the use of the natural bearing capacity of the ground or rock mass. This involves redistributing environmental stresses and using the ground-rock mass as an active support element. This principle was emphasized by Rabcewicz (1964).
2. Flexible Support Systems: NATM recommends the use of flexible and adaptable support systems. These are typically provided by shotcrete, rock bolts, and steel meshes or profiles. The support systems can be adjusted on-site according to the behavior of the ground or rock mass. This approach was detailed by Leca and Panet (1988).
3. Continuous Monitoring: NATM involves the use of continuous monitoring and feedback mechanisms during tunnel excavation. This means the continuous measurement of deformations and stresses, with adjustments to the support systems when necessary. This principle was defined by Schubert and Steindorfer (1996) as a fundamental element of NATM.

In order to design in accordance with the general principles of NATM, it is necessary to examine the behavior of the surrounding rock mass during underground excavation. Deformations in the rock/soil environment begin approximately 1.5 tunnel diameters ahead of the advancing tunnel face, reaching about one-third of the maximum (final) deformation value at the tunnel face. The maximum deformation value is also reached about 1.0 to 1.5 tunnel diameters behind the tunnel face, after which it stabilizes. The deformation pattern of the tunnel is shown in Figure 5.

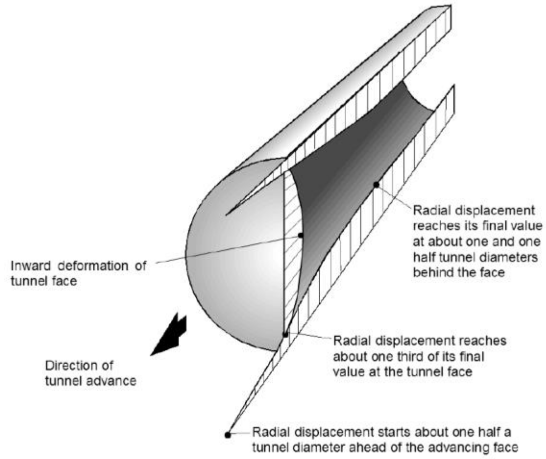

Figure 5. Pattern of deformation in the rock mass surrounding an advancing tunnel (Hoek, 2000)

With these principles, the following analyses and checks were performed in the tunnel design calculations:

- Tunnel Face Stability Analyses and Checks:

It is carried out to determine whether the tunnel face is stable in natural (unsupported) condition and, if it is not stable, to identify the type and number of the support element that ensures stability conditions of tunnel face in excavation direction.

- Tunnel Kinematic Stability Analyses:

It is conducted to perform stability analyses of potential sliding wedges in the radial direction due to rock discontinuities during and after excavation for tunnels to be excavated in a rock environment, and to determine the size, number, and spacing of radial supports (such as soil nails, rock bolts, etc.) that provide sufficient safety factors.

- Two-Dimensional Numerical Analyses and Checks of Tunnel Lining:

It is carried out to check the sufficiency of strength capacities of the tunnel excavation support elements (shotcrete, steel arch composite lining, and soil nails or rock bolts) selected according to KTŞ (2013) under static and seismic loads.

3.1. Tunnel Face Stability Analyses and Verifications

For tunnel face stability, the methods proposed by Cornejo (1989) for tunnels with low cover ($Z \leq 3D$) and by Amberg and Lombardi (1974) for tunnels with high cover ($Z > 3D$) are applied. In tunnel analyses, these two methods are applied according to the following criteria:

Shallow tunnel ($Z \leq 3D$). Tamez & Cornejo Method

Based on the observation that in low cover conditions, the failures at the tunnel face occur in the form of a slip wedge starting from the tunnel face and moving towards the surface, as shown in Figure 6, the stability of wedges 1, 2, and 3 is calculated to verify the stability of the tunnel face. For the stability of the tunnel crown, the stability of wedge 3, as depicted in Figure 6, is considered.

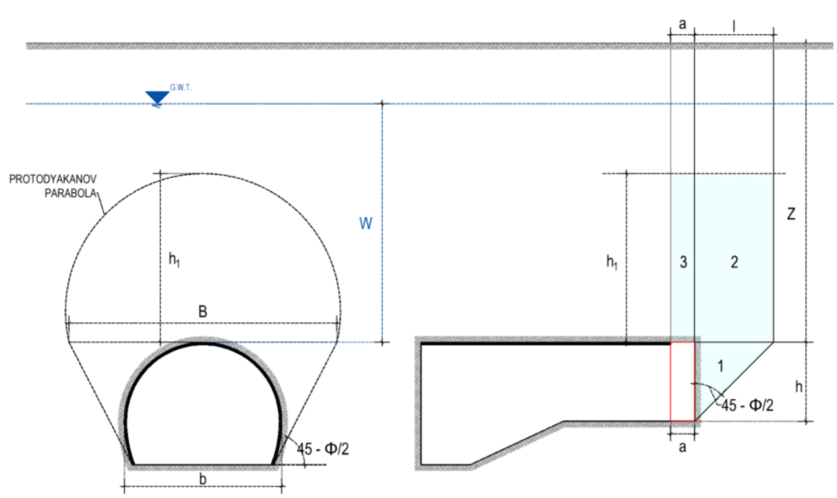

Figure 6. The Notation Used for Tunnel Face Stability Analysis (Cornejo, 1989)

The general safety factor (F_s) of the excavation surface for tunnel face stability and the stability of the tunnel crown (F_{s3}) are expressed by the following equations:

$$F_s = \frac{\left[\frac{2\cdot(\tau_{m2}-\tau_{m3})}{\left(1+\frac{a}{l}\right)^2}+2\cdot\tau_{m3}\right]\cdot\frac{h_1}{b}+\frac{2\cdot\tau_{m3}}{\left(1+\frac{a}{l}\right)\cdot\sqrt{K_A}}\cdot\frac{h_1}{h}+\frac{3{,}4\cdot c}{\left(1+\frac{a}{l}\right)^2\cdot\sqrt{K_A}}}{\left[1+\frac{2\cdot h}{3\cdot Z\cdot\left(1+\frac{a}{l}\right)^2}\right]\cdot[\gamma\cdot Z-P_E]} \tag{1}$$

$$F_{s3} = \frac{2\cdot\tau_{m3}\cdot h_1\cdot(a+b)}{(\gamma\cdot Z-P_E)\cdot a\cdot b} = \frac{2\cdot\tau_{m3}}{\gamma\cdot Z-P_E}\cdot\left[\frac{h_1}{b}\right]\cdot\left[1+\frac{b}{a}\right] \tag{2}$$

When Fs > 2, the tunnel face is stable, and no support is required.
When 1 < Fs < 2, the tunnel face is stable in the short term.
When Fs < 1, the tunnel face is unstable.

Where:

τ_{m2}: The average shear stress acting on the surface of wedge 2

- For shallow tunnels:

$$\tau_{m2} = C+\frac{K_0}{2}\cdot\left[\frac{3{,}4\cdot C}{\sqrt{K_A}}-\frac{(\gamma-\gamma_w)\cdot h}{2}\right] \tag{3}$$

- For deep tunnels:

$$\tau_{m2} = C+\frac{K_0}{2}\cdot\left[w\cdot\gamma+(Z-h_1-w)\cdot(\gamma-\gamma_w)+\frac{3{,}4\cdot C}{\sqrt{K_A}}-\frac{(\gamma-\gamma_w)\cdot h}{2}\right] \tag{4}$$

τ_{m3}: The average shear stress acting on the surface of wedge 3:

- For shallow tunnels:

$$\tau_{m3} = C \tag{5}$$

- For deep tunnels:

$$\tau_{m3} = C+\{0{,}25\cdot[w\cdot\gamma+(Z-h_1-w)\cdot(\gamma-\gamma_w)]-u\}\cdot tan\,\varphi \tag{6}$$

c: Cohesion of the soil inside wedges 2 or 3
a: Excavation length applied by support
l: h x tan(45-ϕ/2)
h_1: Height of the Protodyakonov parabola

- For $h_1 < Z$, $h_1 = B / 2f$
- For $h_1 > Z$, $h_1 = Z$
  - B = b+2h tan (45-ϕ/2)
  - f: Protodyakonov coefficient
    - For Rocks: $f = \sigma_c / 100$
    - For Soils: $f = c / \sigma_c + \tan\phi$

b: Tunnel width
h: Tunnel height
Z: Thickness of the cover layer above the tunnel
k_A: Active thrust coefficient
P_E: Pressure applied to the tunnel face

Deep tunnel (Z > 3D). Amberg and Lombardi Method

The numerical axial symmetric analyses are discussed below. Thanks to the axial symmetric solution method, the two-dimensional finite element model prepared was rotated 360 degrees around the axis to generate a three-dimensional mesh. In the analysis, the stresses that would occur at the tunnel level due to the tunnel face and cover height were modeled, and deformations along the tunnel were observed by excavating up to the equivalent radius of the tunnel face, as shown in Figure 7.

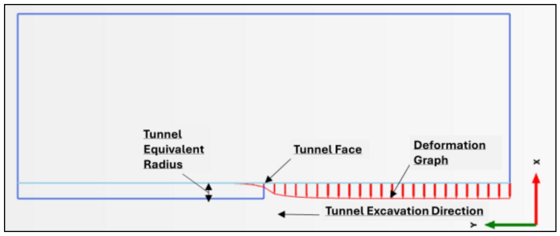

Figure 7. The displacement graph on the representative axial symmetric model.

After the axial symmetric analysis, a two-dimensional material softening analysis was again performed using the Plaxis 2D software. A circular tunnel excavation with the equivalent diameter of the tunnel face was defined on the plane strain model, and stresses caused by the cover height were modeled. The relaxation ratio (deconfinement ratio) of the tunnel face was gradually increased up to 100%, and the deformations corresponding to each relaxation ratio stage were recorded, as shown in Figure 8.

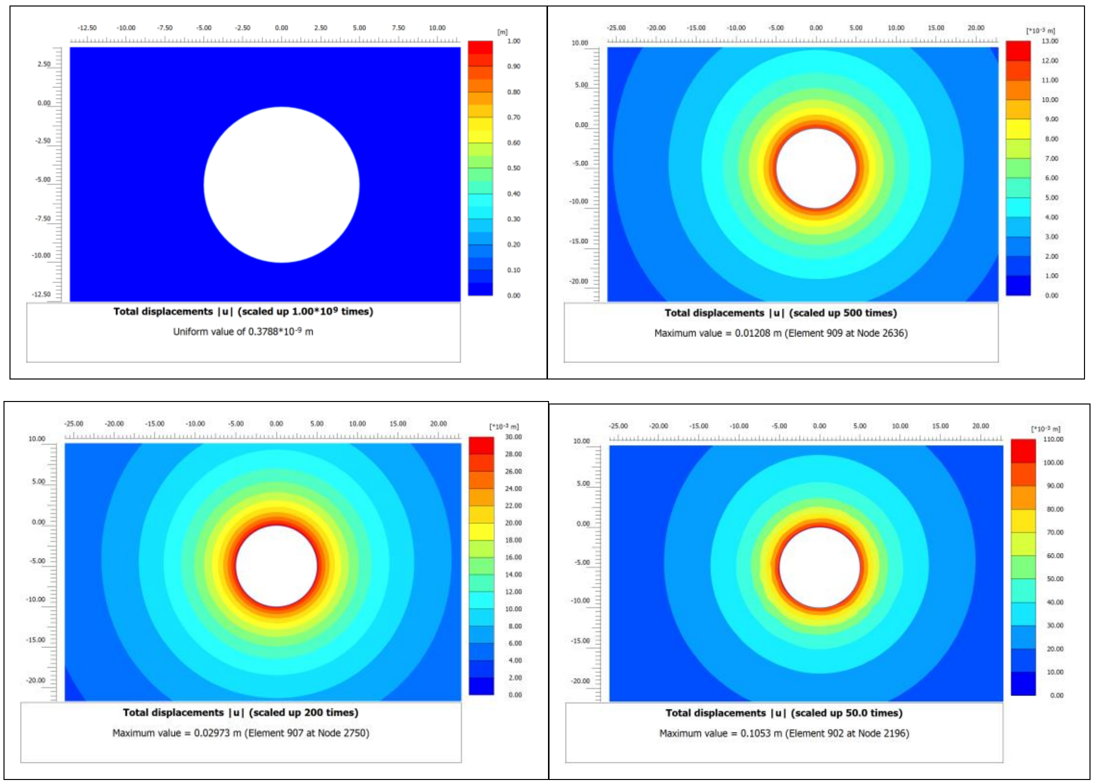

Figure 8. The result of the representative two-dimensional material softening analysis.

As a result of the analysis, the "Ground Reaction Curve" shown in Figure 9 has been plotted. By considering the soil (core region) strength ahead of the tunnel face along with the characteristic curves of the tunnel, the stability of the tunnel face can be evaluated. In the study presented by Amberg and Lombardi (1974), the following formulation was proposed for the soil strength ahead of the tunnel face:

$$R_{core} = c \times k_p^{0.5} \tag{7}$$

$$k_p = tan^2\left(45 + \frac{\varphi}{2}\right) \tag{8}$$

Where:

c: The soil cohesion value at the tunnel face.

k_p: The passive soil thrust coefficient for the soil at the tunnel face.

φ: The internal friction angle of the soil at the tunnel face.

The deformation amount (u_f) corresponding to the calculated core region strength can be obtained from the characteristic curve. For the stability of the tunnel face, an interpretation can be made using Table 3, which was proposed by Amberg and Lombardi (1974).

Table 3. Tunnel Face Behavior Classes (Amberg & Lombardi, 1974)

Behavior Class	$\delta_0 = u_f / R_e$	R_p / R_e
A (Stable)	$\delta_0 \leq \% \ 0,2$	$R_p / R_e \leq 1,1$
B (Short Term Stable)	$\% \ 0,2 < \delta_0 \leq \% \ 0,5$	$1,1 < R_p / R_e \leq 1,5$
C (Unstable)	$\delta_0 > \% \ 0,5$	$R_p / R_e > 1,5$

$$\delta_0 = \frac{uf}{Re} \tag{9}$$

Where:
u_f: The amount of deformation corresponds to the strength of the tunnel core.
R_p: The radius of the plastic zone formed around the tunnel.
R_e: The radius of the equivalent circle of the tunnel excavation area.

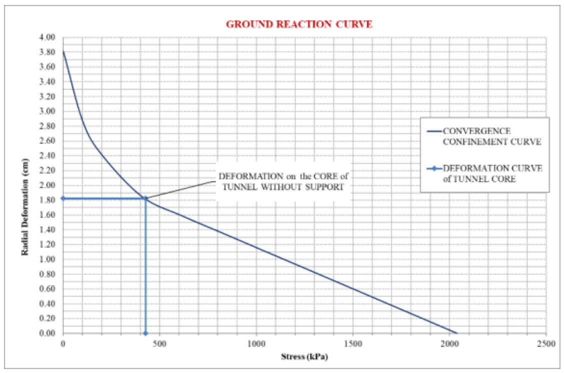

Figure 9. The Representative Ground Reaction Curve Graph.

As a result of the face stability analysis performed in the project, the behavior classes obtained for the unsupported condition of the tunnel face are summarized in Table 4.

Table 4. Tunnel Face Stability Results in Unsupported Condition

Excavation Support Class	Overburden Height	R_e	U_f	$\delta_0 = u_f / R_e$	R_p / R_e	Behavior Class
(-)	(m)	(m)	(cm)	(%)	(-)	(-)
A2	80	5.50	0.53	0.10%	1.00	A (Stable)
B3	85	5.50	1.82	0.33%	1.12	B (Short Term Stable)
C2	85	5.50	2.93	0.53%	1.60	C (Unstable)
B2	60	5.50	0.57	0.10%	1.00	A (Stable)
B1	60	5.50	0.21	0.04%	1.00	A (Stable)
A2	40	5.50	0.11	0.02%	1.00	A (Stable)

For short-term stable or unstable tunnel sections in the unsupported condition, it is envisaged to apply improvement elements for the tunnel face and crown, aiming to achieve a stable behavior class. The results of the stability analysis in the supported condition are summarized in Table 5.

Table 5. Tunnel Face Stability Results in Supported Condition

Excavation Support Class	Support Elements on Tunnel Crown	Support Elements on Tunnel Face	Overburden Height	R_e	U_f	$\delta_0 = u_f / R_e$	R_p / R_e	Behavior Class
(-)	(-)	(-)	(m)	(m)	(cm)	(%)	(-)	(-)
B3	2.5" Forepoling Pipes, Drill Diameter > 80mm, L=6,0m (Overlap Length= 2,25m)	22 Number of Ø28 Soil Nail, Drill Diameter > 100mm, L=9,0m (Overlap Length = 4,0m)	85	5.5	0.90	0.16%	1.00	A (Stable)
C2	48 Number of Ø114/6mm Umbrella Pipes, Drill Diameter > 140mm, L=9,0m (Overlap Length = 5,0m)	35 Number of Ø114/6mm Steel Pipes, Drill Diameter > 140mm, L=9,0m (Overlap Length = 5,0m)	85	5.5	1.00	0.18%	1.10	A (Stable)

3.2. Tunnel Kinematic Stability Analyses

For the Sarıyer-Kilyos Tunnel, the potential wedge-type instability possibilities that could occur parallel to the intersections of rock discontinuities in the tunnel walls have been investigated. Discontinuity measurements were considered for analysis. The contour diagram and stereographic projections of the identified discontinuities have been created with the help of the Dips (2020) software, as shown in Figure 10.

In order to investigate the impact of discontinuity measurements on the tunnel, it has been assumed that the discontinuities have continuity that could intersect the connecting tunnel at any depth. The resulting wedge geometries have been examined using failure criterion proposed by Barton and Bandis (1990) failure criterion.

The predicted wedges formed by the dominant joint sets have been modeled for both static and seismic conditions using the Unwedge (2023) program, as shown in Figure 11.

In light of the conducted analyses, it has been determined that the calculated safety factors are above the required values.

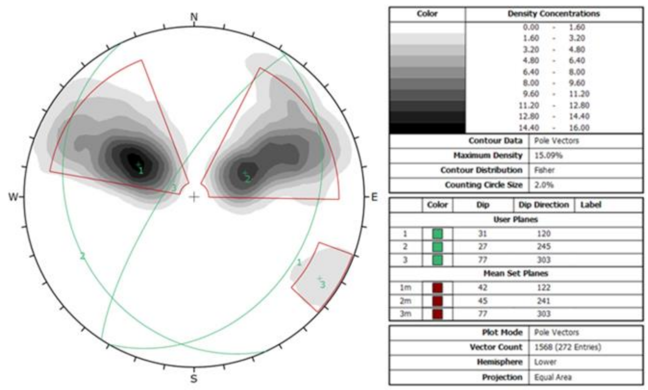

Figure 10. Representative Contour Diagram of Discontinuities for Andesite Units.

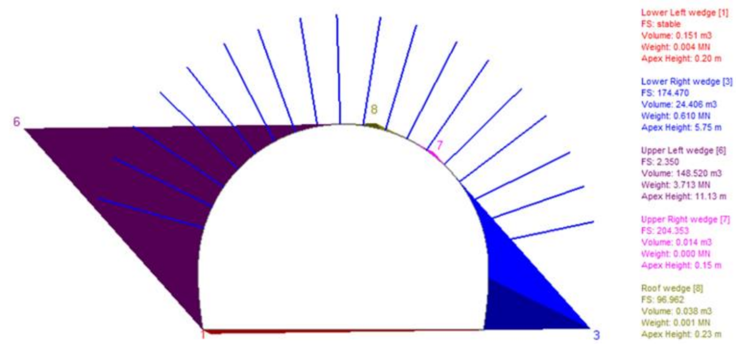

Figure 11. Representative Tunnel Wedge Model

3.3. Two-Dimensional Numerical Analysis and Checks of Tunnel Lining

It is a well-known phenomenon that, as a result of tunnel excavation, the surrounding soil/rock mass reacts with a certain amount of deformation due to the "arching effect," and these deformations vary according to the mechanical properties of the surrounding environment, the overburden height, and the diameter of the tunnel.

In reality, this is a three-dimensional problem, but it can be solved in two dimensions using the "relaxation ratio" approach. The relaxation ratio is determined using axial symmetric analysis for the soil response curve. Through this analysis, radial deformation values along the tunnel profile are determined, and the corresponding relaxation ratio is then calculated using the Plain-Strain Model.

Two-dimensional numerical analysis models were created using Plaxis 2D software. The model consists of the two tunnel cross sections with chosen support systems for both tubes; in order to minimize the effect of the boundary conditions to the calculations the model horizontal limit is taken as minimum 10 diameters of the tunnel for both sides and 5 diameters of the tunnel for bottom limit.

Plain strain type of model used with 15-Noded triangular elements for meshing. Mesh coarseness factor taken as 0.2 around the tunnel, 0.4 at the tunnel level on both sides and 1 for the remaining areas and meshing process done by choosing fine element distribution. The boundary conditions are fixed in x direction and free for y direction on both horizontal limits, fixed in x and y direction at the bottom limit and free in x and y direction on the top of the model. The representative mesh view of the model is shown in Figure 12.

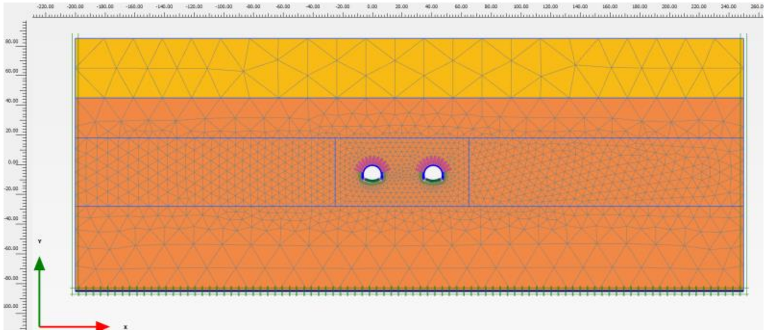

Figure 12. Representative Numerical Model Mesh View

The element number and the node number of the analysis models are summarized in Table 6.

Table 6. Numerical Model Mesh Numbers

Excavation Support Class	Overburden Height	Number of Elements	Number of Nodes
(-)	**(m)**	**(-)**	**(-)**
A2	80	4947	40181
B3	85	3774	30729
C2	85	20042	161385
B2	60	3827	24925
B1	60	3900	28949
A2	40	3360	21843

The numerical modelling of the structural elements is described below:

- The tunnel's temporary lining, consisting of shotcrete and steel ribs, is modeled as "Plate" elements. The element stiffness is defined by the equivalent composite cross-section stiffness.
- The stiffness of shotcrete inside the temporary lining is updated according to the time-dependent curing process of shotcrete during excavation phases.
- Excavation stages, including the overburden, lower bench, and invert, are modeled based on the specified construction phases.
- The tunnel excavation stages are defined and incorporated into the model based on the relaxation ratio and the distance from the tunnel face.
- Rock bolts in the temporary lining are modeled as "embedded beam row" elements.

The results of the analysis, including internal forces on the lining and rock bolts, are verified according to Eurocode "EC2 UNI EN 1992-1-1:2005," and it has been demonstrated in Table 7. that the lining can safely carry the loads applied to it.

Table 7. NATM Support Element Verifications

Excavation Support Class	Calculated Moment on Primary Lining (M_{ed})	Resistance Moment of Primary Lining (M_{Rd})	Factor of Safety for Primary Lining ($Fs=M_{ed}/M_{Rd}$)	Calculated Force on Rock Bolts (N_{ed})	Tensile Resistance of Rock Bolts ($N_{Rd,T}$)	Factor of Safety for Tensile ($Fs=N_{ed}/N_{Rd,T}$)	Pull-out Resistance of Rock Bolts ($N_{Rd,P}$)	Factor of Safety for Pull-out ($Fs=N_{ed}/N_{Rd,P}$)
(-)	**(kNm)**	**(kNm)**	**(-)**	**(kN)**	**(kN)**	**(-)**	**(kN)**	**(-)**
A2	13.73	18	1.31	-	-	-	-	-
B3	141.91	148	1.04	118.3	156	1.32	141	1.19
C2	165.31	197	1.19	131.9	156	1.18	141	1.07
B2	49.84	52	1.04	79.6	106	1.33	101	1.27
B1	27.25	30	1.10	65.1	106	1.63	101	1.55
A2	6.28	10	1.59	-	-	-	-	-

The operational principles of the tunnel lining elements can be listed as in Figure 13.

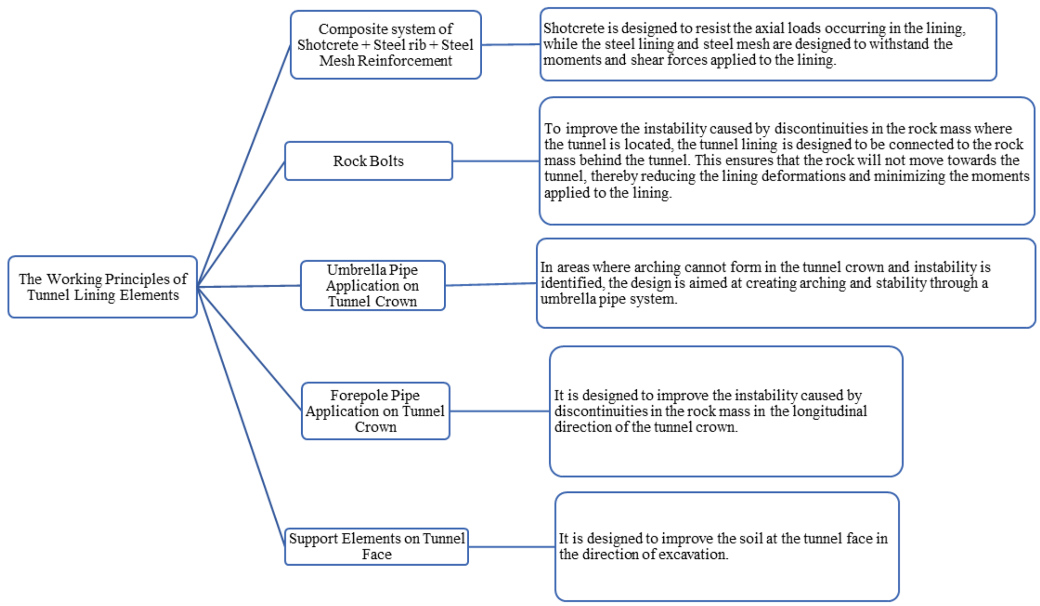

Figure 13. Operational principles of tunnel temporary support systems

As a result of the completed numerical analyses, the support elements for implementation for five different rock classes are provided in Table 8.

Table 8. NATM Support System Elements

Rock Class	Supporting Elements
A2	Double row of Q221 steel mesh, 5 – 6 pieces of Ø28 SN rock bolts, and 10 cm shotcrete.
B1	Double row of Q221 steel mesh, 5 – 6 pieces of Ø28 SN rock bolts, and 10 cm shotcrete.
B2	NPI 160 / 1.5m steel profile, double row of Q221 steel mesh, 11 – 12 pieces of Ø28 SN rock bolts, and 25 cm shotcrete.
B3	NPI 180 / 1.25m steel profile, double row of Q221 steel mesh, 11 – 12 pieces of R32 self-drilling bolts, injection umbrella pipe (if necessary), and 25 cm shotcrete.
C2	NPI 200 / 1.00m steel profile, double row of Q221 steel mesh, 8 pieces of R32 self-drilling bolts, injection umbrella pipe in the tunnel crown and tunnel face, and 30 cm shotcrete.

4. Excavation Methods, Stages and Application of Support Elements

4.1. Excavation Methods and Stages

According to the approved work program as of the date of writing this text, the tunnel excavation method diagram is as shown in Figure 14.

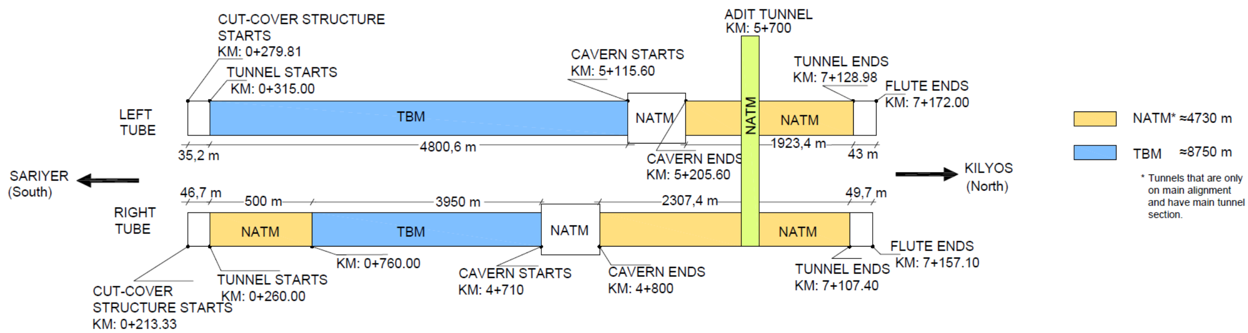

Figure 14. Tunnel excavation method diagram

Following the completion of borehole investigations and in-situ and laboratory assessments, it was determined that the northern (Kilyos) section of the tunnel route is expected to consist of massive or near-massive rock with relatively high Rock Mass Rating

(RMR) values. Consequently, the NATM was chosen and designed for this region. Excavation progress data collected during tunnel construction at the tunnel level confirmed the initial geological projections. Figures 15 and 16 present an example of a face geological mapping form and a tunnel face photograph, respectively.

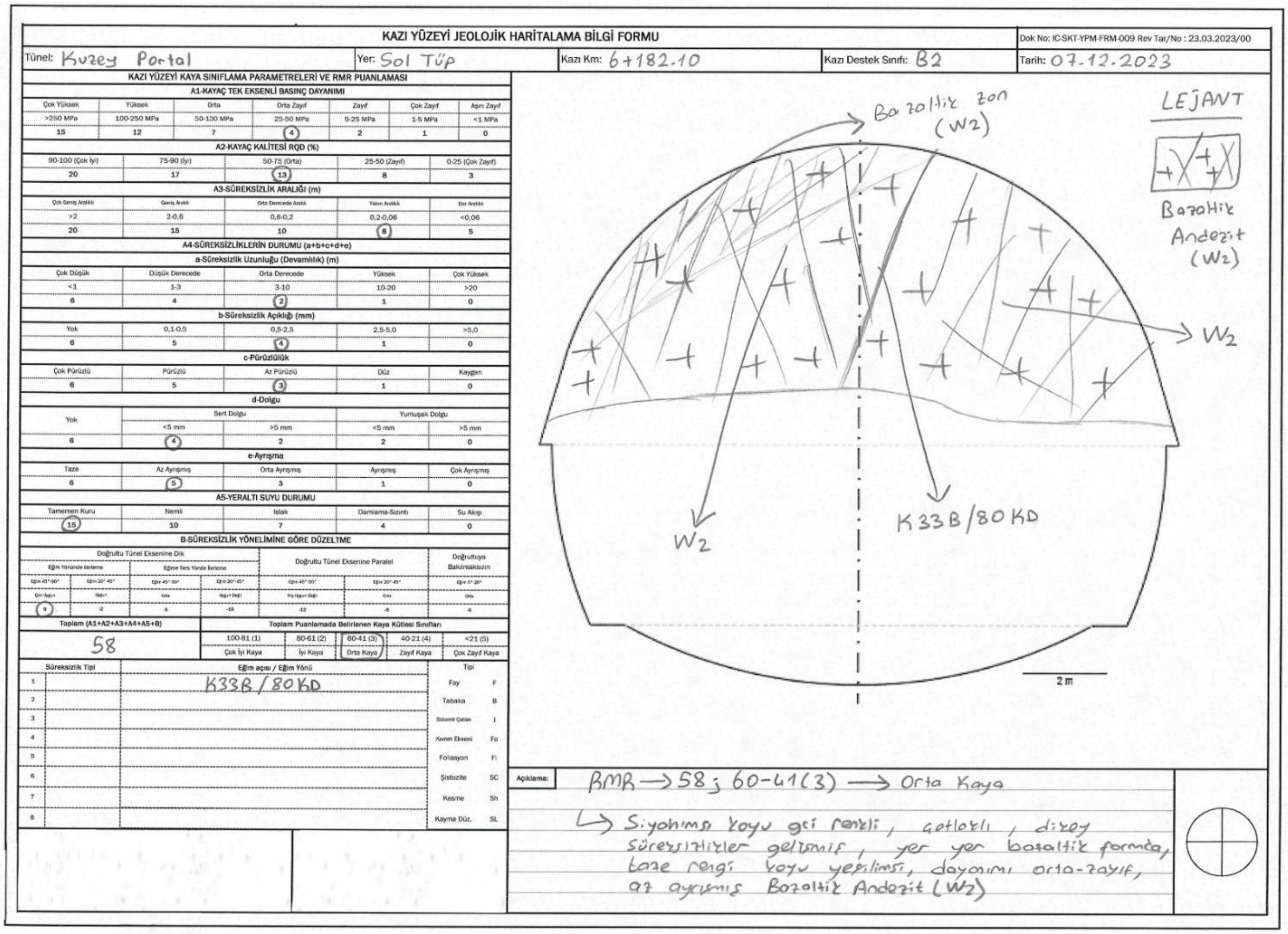

Figure 15. Km: 6+182.10 North left tube

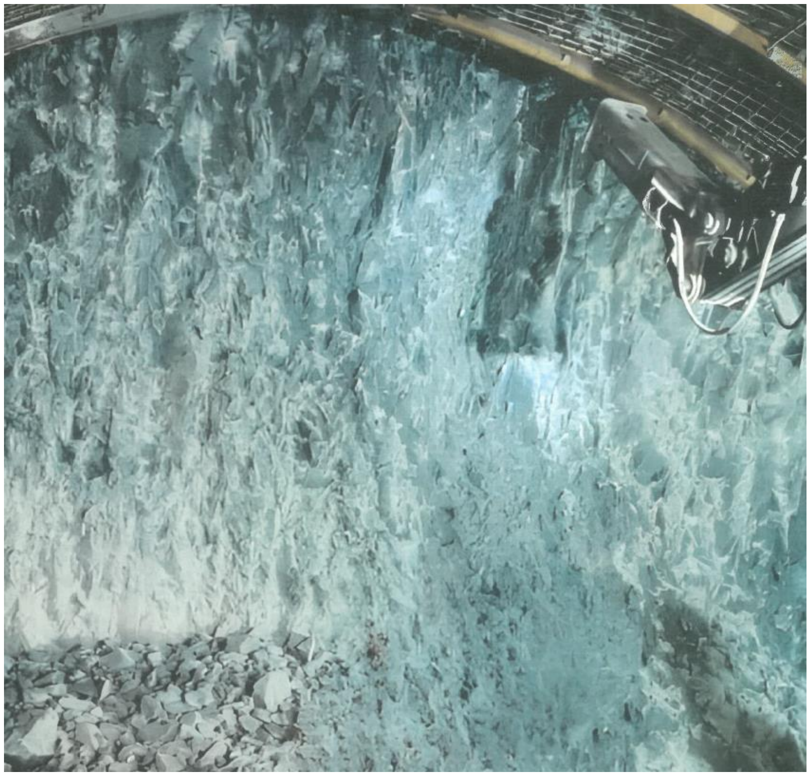

Figure 16. North left tube, Km: 6+182.10

As a result of completing the numerical models of excavation stages and temporary support elements for B1, B2 and B3 classes, no stability issues at the tunnel floor requiring precautionary measures were encountered for all three rock classes. Therefore, on the site, temporary support systems and permanent lining applications for B1, B2, and B3 rock classes were implemented without an invert, while the C2 rock class had a temporary support system without an invert, but permanent lining projects were constructed with an invert.

As detailed in Section 2, the borehole investigations conducted in the northern (Kilyos) region revealed the presence of andesitic rock units belonging to the Garipçe Formation. These formations were also encountered during excavation. Consequently: Excavations in B1, B2, and B3 rock classes were carried out in two stages, comprising a top heading and bench excavation. In the right tube, where the C2 rock class was present, excavation followed a three-stage process, including top heading, bench, and invert excavations, as shown in Figure 17.

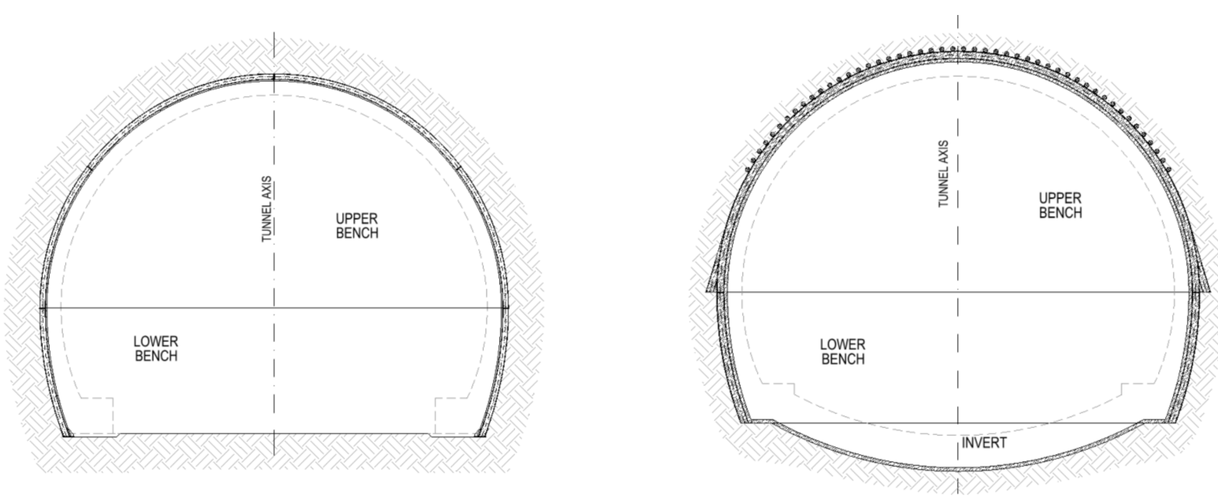

a) b)

Figure 17. **(a)** B1/B2/B3 class excavation sequences **(b)** C2 class excavation sequences

4.2. Blasting Patterns and Site Applications

In Public-Private Partnership (PPP) projects executed under the Build-Operate-Transfer (BOT) tender model, various factors such as environmental and social impacts, quality control/quality assurance requirements, as well as cost and planning constraints, are taken into consideration at every stage of construction. However, in terms of project execution, "construction speed and quality" often take precedence over cost factors. For this reason, in the main tunnels subject to the study area, mechanized excavation was carried out in the C2 rock class for a single advance (12.1 m), whereas all other excavations in B1, B2, and B3 rock classes were completed using the drill-and-blast method. Moreover, the selection of the blasting pattern is significantly influenced by the chosen excavation methods and the geological characteristics of the tunnel alignment. In TBM-excavated tunnels, excavation is performed entirely by the machine, whereas in NATM tunnels, excavation can be conducted using mechanical methods or conventional drill-and-blast. The decision on excavation methodology for NATM was based on comprehensive geotechnical investigations—comprising borehole sampling, in-situ and laboratory testing, and geophysical surveys. Based on the derived physical and mechanical features of rocks and geo-mechanical parameters and considering the proximity of the tunnel alignment to residential and sensitive urban infrastructure, specific excavation methods were selected. For the northern section of the tunnel (Kilyos side), the drill-and-blast method was selected based on several strategic and geotechnical considerations. The tunnel alignment traverses the competent andesite units of the Garipçe Formation beneath a non-urbanized, forested surface zone, offering favorable geological conditions for drill-and-blast excavation. The absence of nearby critical infrastructure further minimized the environmental and social risks typically linked to blast-induced ground vibrations and air overpressure. While mechanized tunneling with appropriate support systems is theoretically feasible in all rock classes, it is essential to conduct a techno-economic evaluation to determine the optimal solution in terms of excavation performance and cost-efficiency. In the northern segment of the referenced tunnel, where rock classes B1, B2, and B3 exhibit relatively high strength and continuity, the drill-and-blast method was preferred. During the determination of blasting patterns, various parameters related to the physical and mechanical properties of the rock were considered., including:

- Rock Mass Rating (RMR) and Rock Quality Designation (RQD),
- Uniaxial compressive strength of the rock,
- Discontinuity characteristics such as location, bedding planes, faulting, folding, length, aperture, roughness, infilling condition (soft vs. hard), and degree of weathering.

Furthermore, in-situ geophysical measurements (e.g., electrical resistivity tomography, multichannel surface wave analysis, and down-hole testing) were utilized to determine shear wave velocities (Vs) and ground properties based on measurements from P- and S-wave velocities.

Along the route, within the section between km 7+100 and 4+500 (applicable for both tubes), the drill-and-blast method was utilized due to the absence of residential areas above the tunnel, the presence of forested terrain, and the relatively high RMR values of massive andesite rock formations belonging to the Garipçe Formation. One of the primary objectives of an effective blasting operation is to minimize adverse environmental effects. Considering such environmental sensitivities, it is essential to limit the instantaneous number of explosives used to prevent adverse effects such as ground shaking, rock ejection or air shock on sensitive areas at a certain distance from the blast source. Accordingly, another crucial aspect of blast design involves determining the maximum permissible number of explosives per delay and ensuring controlled detonations. In the second quarter of 2023, during preparations for tunnel excavation, a requirement arose for the development of a blasting pattern applicable to both the adit tunnel and the main tunnels. To address this need, a team comprising industry-leading experts, academics, and professionals with on-site experience, as well as those involved in sectoral associations, collaborated to establish design methodologies, implementation strategies, and reporting frameworks. The explosive material configuration used in all upper and lower bench-section excavations of B2 and B3 rock classes were as follows:

1. Powergel Magnum 365
2. Excel LP/MS capsule
3. 1.5 Electric Capsule
4. Detonating Cord 10gr

As part of trial-production blasting applications within the tunnel, 10 test blasts were conducted under the supervision of academic team leaders. During these tests, all regulatory measurements, including those from vibration and air shock measurement devices installed within the project site, were performed, and relevant data were collected. These data were subsequently analyzed to evaluate the environmental impacts of blasting operations, considering the relationship between explosive charge amounts and distances in accordance with national and international standards.

Throughout the project, three different vibration measurement devices were utilized, recording a total of 38 events. To estimate peak particle velocity (PPV) due to blast-induced vibrations, the relationship between the scaled distance (SD) (derived from maximum explosive charge per delay and blast distance) and particle velocity data was examined. Based on regression analysis of measured peak particle velocities and scaled distance pairs, vibration propagation formulas for the site were derived for 50% mean prediction and 95% upper prediction limits, as shown below:

50% Mean prediction equation:

$$PPV = 2238.72 \times SD^{-1.865}, r = 0.77 \tag{10}$$

95% Upper prediction equation:

$$PPV = 12531.41 \times SD^{-1.865}, r = 0.95 \tag{11}$$

The blasting patterns used in the study were analyzed in terms of environmental impacts and excavation performance (Kahriman, 2023a). Based on the obtained data and the vibration prediction formula, the expert team developed risk-analysis-based blasting patterns for the main alignment tunnels, considering geological and environmental factors. As a result of these evaluations, two different patterns were proposed for upper bench-section applications, considering the distance of structures identified as potential risk factors: 40-60 meters and 60-100 meters. For the lower bench-section applications, a single pattern was recommended.
Since the tunnel alignment is far from residential areas, the upper bench-section pattern designed for 60-150 meters was applied for B2 and B3 rock classes (Figure 18), while the lower bench-section pattern was applied as shown in Figure 19.

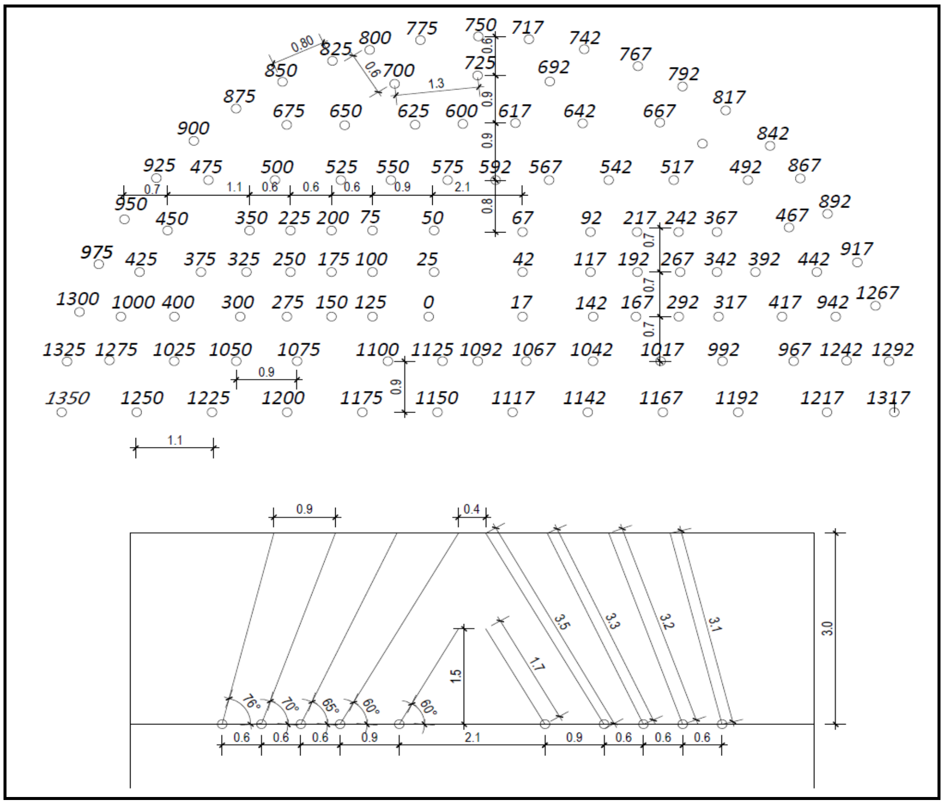

Figure 18. Upper bench blast design

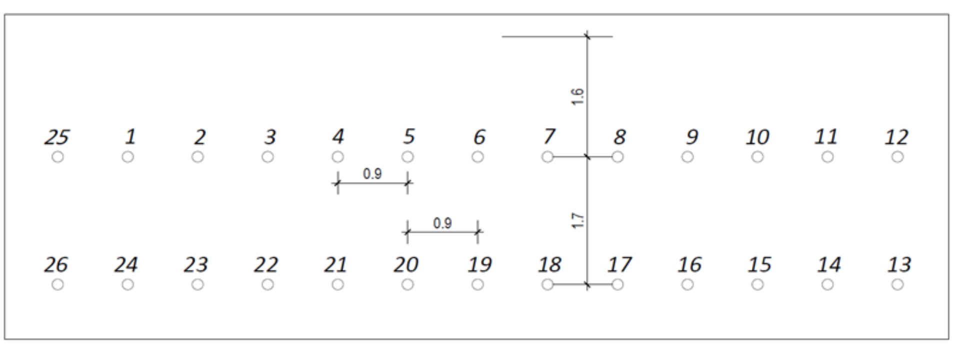

Figure 19. Proposed blasting pattern for the lower bench

For the upper bench-section, the maximum amount of explosive per delay was calculated as 2.6 kg, with a progress length of 3 meters. For the lower bench-section, the maximum amount of explosive per delay was determined as 3.5 kg, with a maximum progress length of 3.5 meters. Although the calculations were completed and the blasting patterns and application methods were developed, as stated in the report's conclusion section, it was noted that "these calculations are of an approximate nature and may be revised based on vibration measurements and excavation efficiency results obtained from test blasts conducted on the site.

As indicated in the report, the implemented blasting pattern was applied for approximately seven months, with minor modifications (such as adjustments to drilling lengths and blast intervals) based on tunnel face mapping studies, which included assessments of formation characteristics, discontinuities, layering directions, and angles. However, excessive overbreak was observed, particularly in the shoulder areas of the tunnel. Figure 20 presents site preparation photographs taken before the blasting process.

a)

b)

Figure 20. (a) Blasting material placement **(b)** Blasting

As a result of the waste calculations and financial impact assessment of the observed overbreak, a commercial and technical evaluation was conducted between the main contractor and the subcontractor at the latter’s request. Based on the guidance of experienced engineers from the main contractor, three solutions were proposed to address the overbreak issues:

- Establishing a control group by reducing drilling depth to 3 meters in a specific section to determine whether the use of 4-meter drilling and conducting two blasts per day genuinely contributed to excessive overbreak.
- Conducting control group blasting trials using 5–6-meter drilling lengths, as seen in international projects where increased excavation speed is a key consideration, to assess the impact on overbreak.
- Identifying operator errors in drilling and, where possible, implementing corrective measures while also reviewing subcontractor claims for additional costs related to excessive overbreak.

Based on these findings, the same expert team conducted a new situational analysis to develop solutions for the overbreak issue. This process involved design, quality, survey, and site teams from the main contractor, who monitored the execution of various work phases over time. Test blasts were performed, evaluations were made, and ultimately, three different blasting patterns were proposed (Kahriman, 2023b).

During various test blasts, several workmanship errors were identified. Some drilling holes, which were supposed to be of equal depth, were found to be either longer or shorter than required, and angular deviations were also observed. Measures were taken to eliminate these execution errors.

While a deviation of 5-10% in drilling hole lengths is generally acceptable in design, site execution errors of up to 40% were detected, which could lead to significant discrepancies.

Failure to achieve uniform drilling depths can reduce the efficiency of explosive usage, cause crater-like formations, and lead to excessive/uncontrolled excavation. Indeed, in test blast areas, it was observed that post-blast scaling and overbreak removal processes took approximately 7 hours to complete. The possible inefficient explosive performance can be seen in Figure 21.

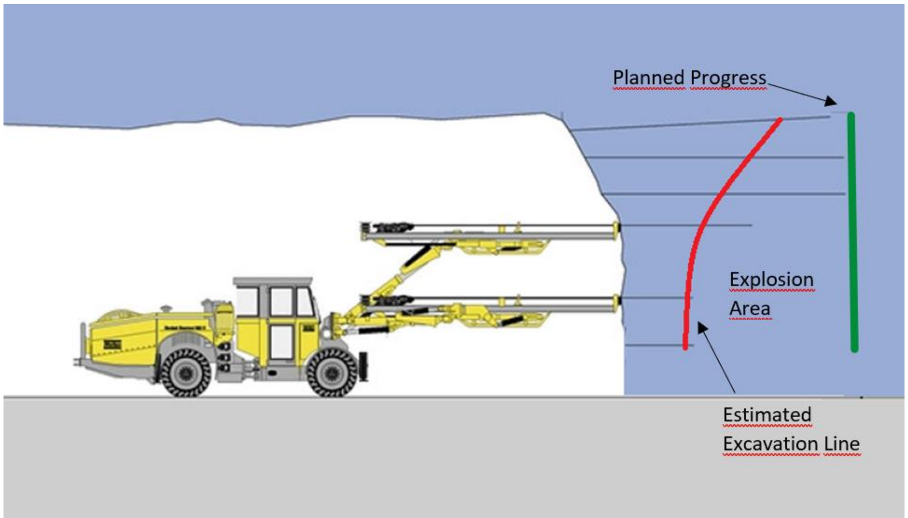

Figure 21. Possible explosion area after blasting

Based on site observations, the expert team considered several critical parameters, including rock quality (mechanical properties), tunnel diameter, proximity to risk points, vibration constraints, and excavation surface sensitivity (Satıcı, 2006). Based on these factors, three excavation patterns were recommended:

1. Blasting with Empty (Burn) Holes (Reduction Hole Based Blasting)
2. Pre-Split Blasting (Pre-cut Applied Blasting)
3. Smooth Blasting (Final Cutting Applied Blasting)

For all three methods, the following specifications were maintained:

- Drill hole diameter: 41-45 mm
- Emulsion explosive: 38 mm in diameter, 400 mm in length, and weighing 500-550 g
- Detonation system: Electric shock tube with millisecond (ms) and long-period (lp) delay detonators
- Design configuration: V-cut (pulling) pattern

Blasting with empty holes

To prevent excessive overbreak, artificial discontinuities were introduced in the tunnel wall by drilling empty relief holes at 30 cm intervals, ensuring that no explosives were placed in these holes.

Additionally, rows of drill holes were arranged with progressively reduced explosive charges from the tunnel center toward the periphery.

Pre-Split blasting

To mitigate excessive overbreak, a pre-splitting line was created 30 cm away from the tunnel excavation boundary in order to create an artificial discontinuity line. Drill holes along this pre-split line were charged with 40 g/m detonating cord and 0.5 kg of emulsion explosive. In shoulder areas, the placement of the detonating cord within the drill holes is illustrated in Figure 22.

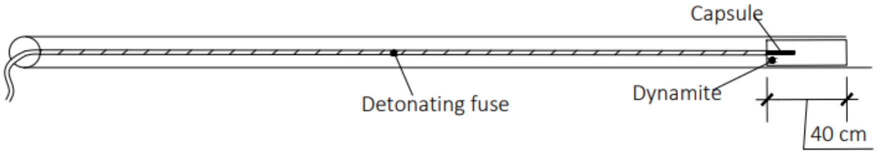

Figure 22. Fuse placement in the hole for pre-split blasting trial

Sequential drill hole rows were arranged in such a way that the explosive charge gradually decreased from the tunnel face center towards the tunnel perimeter.

During the blasting operation, the pre-split line was detonated first to establish a controlled fracture zone along the tunnel perimeter.

Smooth blasting

To prevent excessive overbreak, drill holes along the tunnel perimeter were charged with Trimex explosives, which are designed to reduce the charge concentration within the hole . The arrangment of blasting materials can be seen in Figure 23.
Similar to the pre-split method, sequential drill hole rows were arranged in such a manner that the explosive charge gradually decreased from the tunnel face center towards the tunnel wall. Smooth blasting holes were grouped into different delay intervals to ensure controlled energy release and minimize over-excavation.

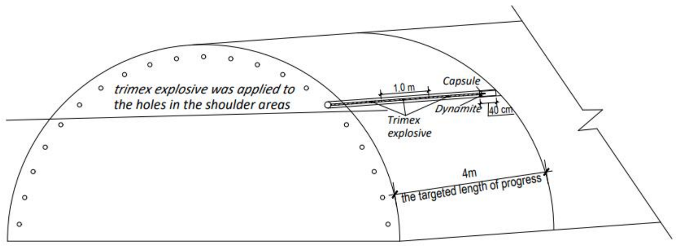

Figure 23. Trimex explosive placement in the hole for the smooth blasting trial.

As a result of the trial blasts conducted for each model, the following assessments were made:
Empty (Burn) Hole-Based Blasting Method (explosive-free, empty holes) was initially recommended by the expert team. Its main advantage is that the excavation line remains closest to the theoretical contour, offering superior performance in preventing overbreak. However, the primary disadvantages are longer overall operation time and higher drilling costs. If the empty hole method is not preferred, smooth blasting is recommended as the second-best option due to its shorter processing time and better excavation accuracy. Pre-split blasting is considered the least favorable model due to its increased preparation time and delay in execution.

As a result of all these model tests, in terms of general evaluation,

The observations of the expert engineers in the site after the test shots are as follows:

- For the B2 rock class in the northern section:
    - The rock exhibited good mechanical properties and low discontinuity frequency. As a result, empty hole method did not perform as expected—unblasted material remained along the contour, requiring additional scaling and localized blasting, leading to time losses.
    - Additional 1 hour was spent for pre-blast drilling, and 7 hours were required for post-blast scaling and clearing operations.
- For the Pre-Split Blasting Model:
    - Along the tunnel perimeter (both shoulders and roof), 40 g/m detonating cord was used within the contour holes.
    - The preparation time increased by 30 minutes compared to other methods.
    - However, this model resulted in a smoother excavation surface, reducing the scaling time to 4 hours and 15 minutes.
- For the Smooth Blasting Model:
    - Trimex cartridge explosives were used for blasting. (both shoulders and roof)
    - The loading process was extended by 1 hour due to the application of trim explosives.
    - The expected smooth excavation was not achieved.
    - Scaling time was recorded as 3 hours post-blasting.

After analyzing trial blast results, expert evaluations, and site observations, the smooth blasting model was decided to be followed and finalized for excavation in B2 and B3 rock classes due to its advantages in post-blast scaling efficiency. Modification of the smooth blasting model: Drill hole lengths, spacing patterns, and explosive quantities were revised on a per-face basis. Although trimex explosives were used in trial blasts, the site team opted for a dynamite-and-capsule-based blasting method for continuous operations.

Upon encountering B1 rock class, the blasting pattern was modified: The smooth blasting model continued to be used, but 40 g/m detonating cord was placed inside contour holes at the shoulders. The main reason for this adjustment was that B1 rock class required thinner shotcrete layers (15 cm) and no steel arches, only double-layer wire mesh reinforcement. Due to the limited thickness of the temporary support system, excessive overbreak could not be tolerated, and a smoother tunnel profile was necessary. Post-blast ventilation took 30 minutes, and scaling and clearing operations were completed in approximately 5 hours. Given the improved excavation accuracy, using detonating cord in contour holes was deemed an effective approach, and the blasting process was continued accordingly.

4.3. Introduction and Application of Support Elements

Based on the numerical analyses introduced in Chapter 3, the support system components implemented in the site are presented in Table 9.

Table 9. NATM Support System Elements

Support Class	Support System elements
B1 rock class	Double-layer Q221 steel mesh, Ø28 SN rock bolt, 15 cm shotcrete
B2 rock class	NPI 160 steel profile, double-layer Q221 steel mesh, Ø28 SN rock bolt, 25 cm shotcrete
B3 rock class	NPI 180 steel profile, double-layer Q221 steel mesh, R32 self-drilling bolt, grouted spiles (if necessary), 25 cm shotcrete
C2 rock class	NPI 200 steel profile, double-layer Q221 steel mesh, R32 self-drilling bolt, grouted umbrella pipes in tunnel crown and face, 30 cm shotcrete

The excavation process began with the upper bench of the tunnel, and the transition to the lower bench was determined based on the rock quality, typically after an advance of 30 to 45 meters. After each round of drilling and blasting, scaling operations were performed to remove loose rock, followed by the application of support elements. Initially, a thin layer of shotcrete was applied to stabilize the rock surface. Then, the first layer of steel mesh was installed, and where required, steel profiles were positioned according to the design specifications. This was followed by the application of a second shotcrete layer, the installation of a final steel mesh layer, and the completion of the shotcrete lining. The rock bolts were installed at a distance of 2 to 5 meters behind the excavation face, depending on the rock class. The same sequence was repeated for the lower bench of the tunnel once the upper bench was stabilized.

For the B3 rock class, fore-polling pipes were installed only, when necessary, whereas in the C2 rock class, grouted umbrellas were applied as a standard procedure. In specific sections of the B2 rock class where fractured, smooth, and unstable rock formations were encountered at the tunnel face, fore-polling were pre-installed before excavation to enhance stability. Similarly, in C2 rock class, grouted umbrella pipes were systematically positioned in the tunnel crown to improve structural integrity before excavation.

During tunnel excavation, rock bolting is implemented to enhance the shear strength of the surrounding rock and to shift the arching effect beyond the excavation boundary (Apaydın et al., 2016). In the site, SN bolts were used in B1 and B2 rock classes, while IBO bolts were applied in B3 and C2 rock classes.

Soil & Nail bolts (SN bolts)

SN bolts are installed in tunnel sections where the boreholes remain stable after drilling. Once drilling is completed, a cement-water grout mixture is injected into the borehole, followed by the insertion of a Ø28 ribbed steel bar, as specified in the project design. After the grout has cured, the bearing plate and nut are tightened, and once the required curing time is achieved, final torque is applied with a wrench to ensure proper anchorage. These bolts serve to connect the initial steel mesh and shotcrete layer to the surrounding rock, effectively counteracting shear forces within rock blocks and enhancing the stability of the tunnel lining.

Self-drilled bolts (IBO bolts)

IBO bolts are preferred for fractured and jointed rock masses where borehole stability cannot be maintained throughout the grouting process. Also known as "self-drilling bolts," IBO bolts feature a drill bit at the tip and a hollow, threaded body. This design allows for simultaneous drilling and installation, eliminating the need for post-drilling bolt placement. Following installation, grout is injected through the hollow core, fully encapsulating both the bolt and the surrounding rock to provide comprehensive reinforcement. SN and IBO bolt applications applied in the site are shown in Figure 24.

a) b)

Figure 24. (a) SN bolt application**. (b)** Self Drilled Rock Bolt application

Forepoling and umbrella pipe

Forepoling and umbrella pipes are installed before excavation in tunnels where there is a risk of ground collapse or water ingress. The primary purpose of these applications is to stabilize the tunnel crown before excavation begins. Forepoling pipes typically have a diameter ranging between 2 to 2.5 inches, whereas umbrella pipes are applied in larger diameters, generally between 3.5 to 4 inches or even larger when necessary. In site applications, the installation of grouted forepoling pipes begins with inclined drilling through the steel arches. Once the pipes are placed, both the interior of the pipe and the surrounding rock interface are completely filled with grout to ensure structural integrity. While the theoretical function of forepoling and umbrella pipes is similar, umbrella pipes are used in more challenging ground conditions where larger deformations are expected. The installation of umbrella pipes starts with drilling boreholes at a 10-degree inclination using an umbrella arc machine. These boreholes are slightly larger in diameter than the pipes themselves to accommodate placement. Perforated pipes are then inserted into the boreholes, and grout is injected to fully fill both the inside and the surrounding voids, ensuring proper reinforcement. Figure 25 illustrate examples of forepoling and umbrella pipe installations in the site.

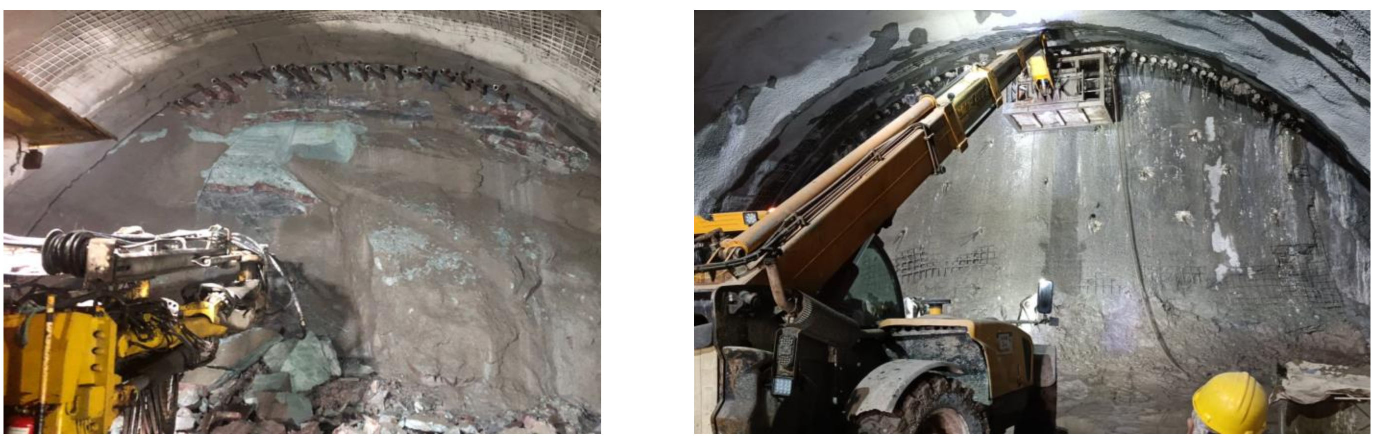

a) b)

Figure 25. (a) Umbrella Pipe Application. **(b)** Umbrella Pipe application

4.4. Temporary and Permanent Drainage System Installations

Temporary drainage

According to the Highways Technical Specification 2013, Section 350.03.02.09, three different drainage systems are defined to manage water ingress during tunnel construction, preventing water accumulation that could obstruct excavation activities.

1. Longitudinal Drainage: This system consists of gravel-filled trenches placed along the excavation base. In areas with high water inflow, perforated rigid PVC pipes with diameters ranging from 150 to 200 mm may be installed to handle the excess water.

2. Radial Drains: In locations with significant water flow, inclined drainage holes are drilled into the rock mass. Inside these holes, perforated steel or rigid PVC pipes with a 1.5-inch diameter are installed—perforated along the upper section and sealed at the lower section. These pipes are positioned at the tunnel crown and shoulders. The pipe openings are sealed with quick-setting mortar and connected to the longitudinal drainage system, sump pits, or collection trenches at the tunnel base.
3. Peripheral Drains: In wet rock surface areas, water is collected using semi-circular drainage channels (preferably corrugated flexible PVC pipes) that are fixed to the rock with quick-setting mortar or shotcrete. These drains are then connected to sump pits or longitudinal trenches at the excavation base.

During the construction of the Sarıyer-Kilyos Tunnel, borehole drilling and subsequent pumping tests predicted minimal water ingress in the northern section (Kilyos), where the NATM tunnels were excavated. This forecast was confirmed upon the completion of temporary support structures, as no significant water accumulation or excessive inflows were encountered. Water discharge during tunnel excavation was managed through drainage channels along both tunnel sides, from which water was pumped out to the surface.

Permanent drainage

Once excavations are completed and temporary support structures are installed, an effective drainage system must be implemented before the final lining is constructed. This system is essential to prevent groundwater accumulation behind the permanent lining throughout the tunnel's operational lifespan. Effective drainage is crucial to mitigating unforeseen water pressure on the final lining and prolonging its structural durability.

The permanent drainage system installation must commence alongside the casting of the base beams, which form the foundation of the final lining. Preventing water buildup behind the lining is vital to avoiding premature deterioration and excessive hydrostatic pressure, which could compromise the structural integrity of tunnel components. The drainage components used for B1, B2, and B3 rock classes without permanent invert lining are illustrated in Figure 26.

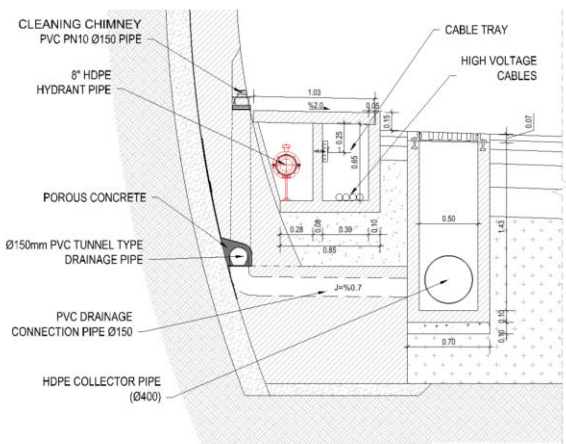

Figure 26. Permanent drainage system

To prevent water accumulation behind the tunnel lining, side drainage systems are implemented. The first step in this process involves installing 150mm PVC tunnel pipes, which are then encased in porous concrete. Before laying the felt and membrane layers, all protruding surfaces (such as binding wires and exposed reinforcement elements within the permanent structure) are scanned and smoothed using a final layer of shotcrete with finer aggregate particles compared to standard shotcrete applications. This precaution prevents potential membrane punctures during the subsequent stages of lining installation.

5. Conclusion

Construction of the Northern Marmara Motorway Odayeri – Paşaköy Section (including the Third Bosphorus Bridge), which spans over 450 km, commenced to construction in 2013, and sections of it were progressively opened for public use from August 26, 2016. This infrastructure has provided a fast, reliable, and comfortable transportation corridor between Anatolia, Asia Minor and Europe. In addition to connecting the two continents, the motorway significantly alleviates urban traffic congestion by facilitating transit routes in the cities it passes through. As part of the broader Northern Marmara Motorway project, essential intercity connections, particularly in Istanbul, have been developed, with most of them now completed.

The Sarıyer-Kilyos Tunnel and its connection roads aim to reduce congestion along the Bosphorus corridor, providing a five-minute direct link between Sarıyer County Center and the Northern Marmara Motorway. This tunnel seamlessly integrates with the international Trans-European North-South Motorway (TEM) Project and offers efficient access to major urban transportation hubs, including Istanbul New Airport and Sabiha Gökçen Airport.

Istanbul, home to Türkiye's largest population segment, is projected to experience significant population growth. According to officially published projections in the Istanbul Metropolitan Municipality Dataset, the city's population is expected to reach approximately 48,476,480 by 2050 under the first projection scenario. With increasing urbanization, traffic congestion will become an even greater challenge, highlighting the indispensable role of the Sarıyer-Kilyos Tunnel in addressing mobility and infrastructure needs. As a major Build-Operate-Transfer (BOT) project, this tunnel serves as an exemplary collaboration between the General Directorate of Highways (KGM) and the private sector. From a design, construction, and operational perspective, it introduces significant advancements to the tunneling industry.

Prior to construction, geotechnical investigations and borehole analyses were conducted to predict the distribution of rock classes along the tunnel route. The estimated percentage breakdown of NATM support classes is provided in Table 10. However, as of the writing of this document, the actual excavation process has predominantly encountered B2 rock class, along with B1, B3, and single-phase C2 rock formations.

Table 10. Designed NATM temporary support class rates before application of project

Right and Left Tube Total	A2 Excavation Support	B1 Excavation Support	B2 Excavation Support	B3 Excavation Support	C2 Excavation Support
Designed classes	14.2%	9.7%	17.9%	49.1%	9.0%

Examining these figures reveals a common characteristic of NATM tunneling preliminary geotechnical analyses based on borehole data may not always accurately predict the actual rock classes encountered during excavation. This underscores the critical importance of continuous tunnel face mapping studies throughout each excavation step of all the construction process.

The study demonstrates that the blasting pattern and temporary support elements might be modified/redesigned at each excavation step according to location, spacing, and angle of discontinuity, bedding plane, weathering degree, etc., even if the excavation proceeds in the same rock class.

Based on observed overbreak and the geological variability encountered during excavation, combined with detailed test blasts at the primary tunnel site, several strategic refinements were proposed to address over-excavation effectively:

- Equal length hole drilling allows for efficient use of explosives. Progress of 4-5 meters per blast is appropriate, and larger advances should not be targeted.
- If the empty (burn) hole-based blasting model is followed, it is recommended to reduce the hole spacing and loading distance for the contour holes, reduce the charge amounts of the contour holes, and reduce the charge of the stopping holes immediately in front of the contour holes.
- In the case of B2 class rock with good mechanical properties and few discontinuities, as in the example of the study area, the empty hole blasting model fails to achieve the expected excavation performance, and significant time is spent on post-blast trimming/material retrieval.
- For B2 class rock with few discontinuities, the smooth blasting method using dynamite and capsules together in the shoulder regions, with optimized hole lengths, explosive amounts, and post-blast trimming/material removal advantages, is recommended.
- In B1 class rock, due to the lower thickness of the temporary support system, excessive excavation after blasting cannot be tolerated. Therefore, the required smooth blasting surface is recommended to be achieved by placing explosive cords in the shoulder holes along the tunnel axis, using the smooth blasting model.

By implementing these strategies, the Sarıyer-Kilyos Tunnel project has successfully addressed over-excavation challenges while ensuring efficient tunnel stability and construction progress.

5.1. References

Alğın, H. M., Ekmen, A. B., & Yenmez, L. (2019). Three-Dimensional Finite Element Analysis of Piled Raft Foundations. Technical Journal, 30(5), 9443–9458. https://doi.org/10.18400/tekderg.399679

Amberg, W. A., Lombardi, G. (1974). Une méthode de calcul élstoplastique de l'état de tension et de déformation autour d'une cavité souterrain. Proc. 3rd Congr. Int. Soc. Rock Mech.,Vol. 2B, 1055–1060.

Aral, I.O., Tüysüz, O., (1999). Tethyan Sutures of Northern Turkey, Geological Society, v.156, 475-515, doi:10.1144/GSL.SP.1999.156.01.22

Avcı, Y., Ekmen, A. B., (2023). Artificial intelligence assisted optimization of rammed aggregate pier supported raft foundation systems based on parametric three-dimensional finite element analysis. Research Journal of The Institution of Structural Engineers, Vol. 56. https://doi.org/10.1016/j.istruc.2023.105031.

Barton, N., & Bandis, S. (1990). Review of predictive capabilities of JRC-JCS model in engineering practice. Proc International Symposium on Rock Joints, 28(4), 209. doi: 10.1016/0148-9062(91)90682-C.

Baş, S. (2019). Estimation of Seismic Response of R/C Frame Structures to Vertical Earthquake Motion Considering Fixed Support and Soil-Structure-Interaction (SSI). International Journal of Engineering Research and Development, 11(1), 7-17. https://doi.org/10.29137/umagd.482482

Cornejo, L. (1989). Instability at the face: its repercussion for tunnelling technology. 21(4), 69-74

Çoruh, E., Köksal, A. O., Kaplan, C., & Demirci, M. (2017). Construction Activities and Methodology of the Kop Tunnel. Journal of Science and Technology of Ordu University, 7(2), 275–288.

Çümen, Ö. F., & Karakaş, A. (2021). Engineering Geological Investigation of the Kırık Tunnel Route. Kocaeli Journal of Science and Engineering, 4(2), 93-102. doi: 10.34088/kojose.904895.

Dips V.7.018, (2020). Program Designed For The Interactive Analysis Of Orientation Based Geological Data. Rocscience Inc.

Ekmen, A.B., Avci, Y. (2023). Artificial Intelligence-Assisted Optimization of Tunnel Support Systems Based on the Multiple Three-Dimensional Finite Element Analyses Considering the Excavation Stages. Iran J Sci Technol Trans Civ Eng 47, 1725–1747. https://doi.org/10.1007/s40996-023-01109-7

Eurocode 2: Design of concrete structures – Part 1-1: General rules and rules for buildings. (1992). Brussels, European committee for standardization

Furat, B. Ö., & Bulut, F. (2020). A Geotechnical and Support System Assessment of the Entrance and Exit Sections of the Right Tube of the Güneyce Highway Tunnel. Bulletin of the Chamber of Geological Engineers, 44(1), 1–18. https://doi.org/10.24232/jmd.740503

Hiçyılmaz, Ö. S., & Özçelik, M. (2019). Construction Activities of the T-5 Tunnel within the Ankara–Sivas High-Speed Railway Project. Journal of Engineering Sciences and Design, 7(2), 321–329. https://doi.org/10.21923/jesd.491825

Hoek, E. (2006), Practical Rock Engineering. Evert Hoek Consulting Engineer Inc.

Kahriman, A. (2023a). Blasting Excavation Design Report Based on Vibration Analysis for the Sarıyer–Kilyos Highway Tunnel Construction Project.

Kahriman, A. (2023b). Evaluation of Drilling and Blasting Models Implemented in the Tunnels of the Sarıyer–Kilyos Project.

Kahyaoğlu, H. (1998). Tunnel Works and the New Austrian Tunneling Method (NATM) with Reference to the TAG Motorway. In 4th Transportation Congress of the Chamber of Civil Engineers, pp. 49–64.

General Directorate of Highways. (2013). Highway Technical Specifications. Ankara, Türkiye: General Directorate of Highways.

Leca, E., & Panet, M. (1988). Analytical and Numerical Analysis of the Convergence-Confinement Method for Tunnel Design. Rock Mechanics and Rock Engineering, 21(2), 119-132.

Önorm B 2203-1. (2001). Vienna, Austrian Standards Institute.

Plaxis 2D V.21.01., (2021). Finite Element Program, Developed For The Analysis of Deformation, Stability And Groundwater Flow in Geotechnical Engineering. Plaxis bv, Bentley Systems Inc.

RocLab V.0.1., 2007. Rock Mass Strength Analysis using the Generalized Hoek-Brown Failure Criterion. Rocscience Inc.

Rabcewicz, L. (1964). The New Austrian Tunnelling Method, Part One. Water Power, 453–457.

Satıcı, Ö. (2006). Drilling and Blasting as a Tunnel Excavation Method. Researchgate. https://www.researchgate.net/publication/285057196_Drilling_and_blasting_as_a_tunnel_excavation_method?channel=doi&linkId=565b86c708aefe619b243d4d&showFulltext=true

Schubert, W., & Steindorfer, A. (1996). Advanced monitoring data evaluation for tunnels in poor rock. In Prediction and Performance in Rock Mechanics and Rock Engineering, Proceedings EUROCK ´96, Vol. 2 (pp. 1041-1046).

Singh S. P., Xavier, P. (2004). Causes, impact and control of overbreak in underground excavations. Tunnelling and Underground Space Technology, 20(2005) 63-71.

UnWedge V.5.017, (2023). Program Designed for The Analysis of The Geometry and Stability of Underground Wedges Defined by Intersecting Structural Discontinuities in The Rock Mass Surrounding an Underground Excavation. Rocscience Inc.